OL | Organic Letters

Letter

Cite This: Org. Lett. 2019, 21, 4554–4558

pubs.acs.org/OrgLett

Four Yellow Monoterpenoid Quinoline Alkaloids from the Stem of *Tabernaemontana bovina*

Jing Wu,[†,‡] Yang Yu,[†,‡] Yi Wang,[§] Mei-Fen Bao,[†] Bao-Bao Shi,[†,‡] Johann Schinnerl,[∥] and Xiang-Hai Cai*[,†]

[†]State Key Laboratory of Phytochemistry and Plant Resources in West China, Kunming Institute of Botany, Chinese Academy of Sciences, Kunming 650201, China

[‡]University of Chinese Academy of Sciences, Beijing 100049, China

[§]Bristol-Myers Squibb Co., Lawrenceville, New Jersey 08648, United States

[∥]Chemodiversity Research Group, Division of Systematic and Evolutionary Botany, University of Vienna, Rennweg 14, A-1030 Vienna, Austria

Supporting Information

ABSTRACT: Four unprecedented yellow alkaloids named as taberbovines A–D (**1**–**4**) were isolated from stems of *Tabernaemontana bovina* Lour. Their structures were elucidated by the comprehensive spectroscopic data, computational chemistry, and X-ray crystal diffraction. Alkaloids **1**–**4** possessed a unique 6/6/5/6/5 ring system and were assigned to monoterpenoid quinolines. Biosynthetically, the isolated alkaloids may be derived from *Aspidosperma*-type alkaloid by oxidation and rearrangements. Taberbovines A–D exhibited the good inhibitory activities of formation NO in LPS induced RAW264.7 macrophages.

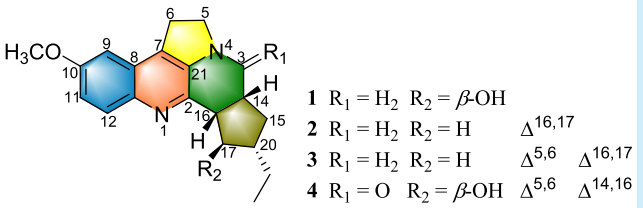

Alkaloids are unique natural products denoted by the presence of at least one nitrogen atom as part of a heterocyclic ring, constituting a highly diverse group of secondary metabolites. To date, approximately 15 000 structurally different alkaloids are known from natural sources. This class of secondary metabolite is divided in dozens of subgroups according to their carbon skeleton.[1] Among them, monoterpenoid indole alkaloids (MIAs) may account for a quarter of naturally occurring alkaloids. Their highly intricate chemical structures and pronounced pharmacological activities attracted a great deal of attention from researchers interested in their structural diversity, bioactivities, and (bio)synthetic pathways.[2] Generally, MIAs are classified as *Corynanthe*, *Strychnos*, *Yohimbine*, *Iboga*, and *Aspidosperma* types according to the structural modifications of the monoterpenoid moiety which is derived from the iridoid secologanin. The monoterpenoid quinoline alkaloids (MQAs) are derived from MIAs. Camptothecin, quinine, scandine, ochroborine A,[3] and meloyunine C[4] are representatives of MQAs. They are formed by the oxidative cleavage of C–2/7, leading to a new ring system with a C–2/6 bond. MIAs and MQAs include several colorful compounds such as camptothecins, ellipticine, melodinine M,[5] and ochropposine.[6] These compounds usually possess additional conjugated double bonds besides the original indole or quinoline moiety, which further leads to differences in the absorption of UV–vis light. These differences suggest distinctions in either the arrangement of conjugated double bonds or even structural types.

The pantropical distributed genus *Tabernaemontana* (Apocynaceae)[7] is known as a rich source of structurally complex MIAs, such as the tetrakis.[8] Commonly, MIAs usually possess UV absorption bands at 220 and 280 nm. Herein, we describe four novel MQAs, named as taberbovines A–D (**1**–**4**) isolated from the stem of *T. bovina* Lour.[9] All of them possess new skeletal motifs featuring a multiring system (Figure 1).

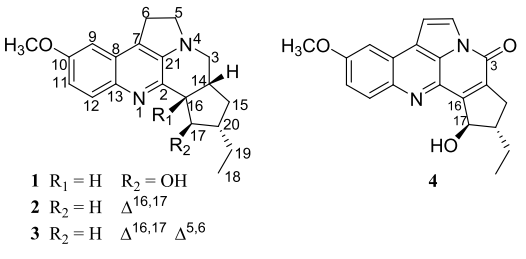

Figure 1. Structures of alkaloids taberbovines A–D (**1**–**4**).

Crude alkaloid of *T. bovina* (Supporting Information, SI) was subjected to column chromatography. All of the collected fractions were analyzed by HPLC-PDA, and each peak of the UV spectra was compared to those of known MIAs. Fraction V (4.8 g) containing compounds with campothecin-like UV spectra (Figure 2) was further separated by reversed-phase

Received: April 26, 2019
Published: June 10, 2019

DOI: 10.1021/acs.orglett.9b01453
Org. Lett. 2019, 21, 4554–4558

MPLC, HPLC over a C18 column, yielding compounds **1**–**4** (SI).

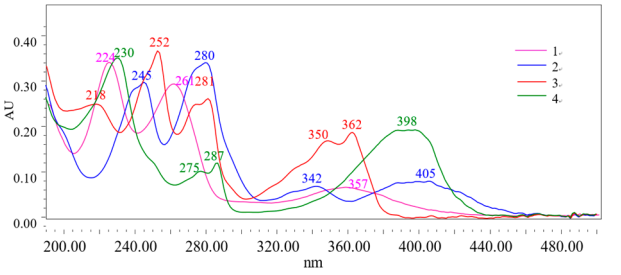

Figure 2. UV–visible absorption spectra of alkaloids **1**–**4**.

Compounds **1**–**4** were yellow-colored alkaloids and exhibited a positive reaction with Dragendorff's reagent on TLC. The UV absorption bands at 224, 261, and 357 nm of **1** were similar to those of 10-methoxycamptothecin,[10] which indicated the presence of a quinoline core structure. Compound **1**[11] possessed a molecular formula $C_{20}H_{24}N_2O_2$ as established by the HRESIMS (m/z 325.1911 $[M + H]^+$), indicating 10 degrees of unsaturation. The ^{1}H NMR spectra of **1** exhibited a 10- or 11-substituted quinoline from three coupling benzene proton signals [δ_H 7.80 (1H, *d*, J = 9.1 Hz), 7.08 (1H, *dd*, J = 9.1, 2.8 Hz), 7.00 (1H, *d*, J = 2.8 Hz)]. Its ^{13}C and DEPT spectra (Table 1) showed 20 carbon resonances belonging to six quaternary carbons (δ_C 158.5, 147.1, 145.3, 141.3, 129.1, 127.8), seven methines (δ_C 131.4, 118.5, 101.4, 83.2, 49.3, 48.7, 35.8), five methylenes (δ_C 56.5, 53.6, 33.8, 28.1, 27.2), one methyl (δ_C 12.7), and one methoxyl (δ_C 55.7) group. The ^{1}H and ^{13}C NMR patterns of **1** were similar to those of 10-methoxycamptothecin.[12] The single methoxyl group could be located at C-10 rather than C-11 based on the HMBC correlations from H-9 (δ_H 7.00) to C-11 (δ_C 118.5 d)/C-13 (δ_C 141.3, s), and from the methoxyl as well as H-12 (δ_H 7.80) to C-10 (δ_C 158.5). The correlations between H-9 and the signal of δ_C 129.1 (s) assigned this carbon signal to C-7. Similarly, the methylene protons (δ_H 3.27, 3.20) showed the HMBC cross-peaks to C-8 (δ_C 127.8 s), assigning themselves to be CH_2–6 which was connected to C-7. Subsequently, the methylene protons (δ_H 3.60 and 3.31) showed coupling with H-6 in the ^{1}H–^{1}H COSY spectrum, being assigned to CH_2–5 and exhibiting connectivity with N-4 in consideration of its corresponding carbon chemical shifts (δ_C 56.5 t) in the HSQC spectrum (Table 1). Both the H-6 and H-5 showed cross-peaks to the upfield signal (δ_C145.3, s), suggesting the presence of a pyrrole ring (C_{21}–C_7–C_6–C_5–N_4) (Figure 3, Unit A). In the ^{1}H–^{1}H COSY spectrum of **1**,

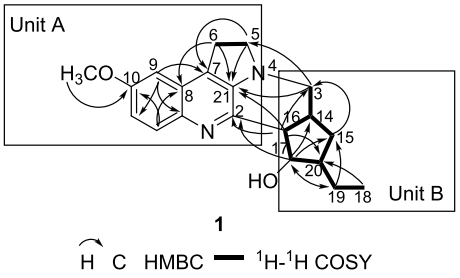

Figure 3. Key HMBC and ^{1}H–^{1}H COSY correlations of alkaloid **1**.

cross-peaks of δ_H 0.93 (H-18)/δ_H 1.66 (H-19)/δ_H 1.88 (H-20)/δ_H 3.72 (H-17)/δ_H 3.04 (H-16) constructed C_{18}–C_{19}–C_{20}–C_{17}–C_{16} connectivity. Similarly, cross-peaks of δ_H 1.88 (H-20)/δ_H 2.28 (H-15)/δ_H 2.88 (H-14)/δ_H 3.11 (H-3) gave a

Table 1. ^{1}H and ^{13}C NMR Spectroscopic Assignments of 1–4 in Acetone-d_6 (J in Hz)

no.	δ_H (1)	δ_C (1)	δ_H (2)	δ_C (2)	δ_H (3)	δ_C (3)	δ_H (4)	δ_C (4)
2		147.1 s		147.0 s		138.9 s		135.7 s
3	3.11 (dd, 10.6, 5.1)	53.6 t	3.52 (dd, 9.7, 5.1)	54.8 t	4.74 (dd, 11.6, 6.3)	51.4 t		158.4s
	2.51 (dd, 10.6, 4.6)		2.44 (dd, 9.7, 3.9)		3.78 (t, 11.6)			
5	3.60 (m)	56.5 t	3.81 (overlap)	55.8 t	7.47 (d, 2.8)	128.9 d	8.08 (d, 3.4)	124.9 d
	3.31 (m)		3.16 (overlap)					
6	3.27 (m)	28.1 t	3.33 (m)	28.3 t	7.01 (d, 2.8)	101.6 d	7.52 (d, 3.4)	109.6 d
	3.20 (m)		3.16 (overlap)					
7		129.1 s		128.5 s		129.1 s		128.1 s
8		127.8 s		128.9 s		125.9 s		126.3 s
9	7.00 (d, 2.8)	101.4 d	6.92 (d, 2.8)	101.0 d	7.61 (d, 2.9)	103.6 d	7.85 (d, 2.8)	103.3 d
10		158.5 s		158.9 s		158.4 s		160.4 s
11	7.08 (dd, 9.1, 2.8)	118.5 d	7.03 (dd, 9.2, 2.8)	118.7 d	7.16 (dd, 9.1, 2.9)	117.5 d	7.44 (dd, 9.2, 2.8)	121.2 d
12	7.80 (d, 9.1)	131.4 d	7.75 (d, 9.2)	132.0 d	7.99 (d, 9.1)	131.7 d	8.20 (d, 9.2)	133.1 d
13		141.3 s		141.2 s		139.6 s		142.6 s
14	2.88 (overlap)	35.8 d	3.33 (overlap)	45.2 d	3.54 (m)	44.6 d		139.5 s
15	2.28 (m)	33.8 t	2.42 (dd, 11.8, 2.9)	37.2 t	2.58 (dt, 12.1, 7.2)	36.5 t	3.21 (dd, 16.8, 8.0)	34.9 t
	1.20 (overlap)		1.18 (dd, 11.8, 10.3)		1.32 (dt, 12.1, 9.7)		2.50 (dd, 16.8, 6.6)	
16	3.04 (t, 8.3)	49.3 d		137.7 s		138.0 s		152.8 s
17	3.72 (t, 8.3)	83.2 d	6.49 (d, 2.3)	130.8 d	6.77 (d, 2.3)	133.3 d	5.47 (m)	80.8 d
18	0.93 (3H, t, 7.4)	12.7 q	1.00 (3H, t, 7.4)	12.4 q	1.03 (3H, t, 7.4)	12.4 q	1.12 (3H, t, 7.4)	12.7 q
19	1.66 (m)	27.2 t	1.61 (m)	29.7 t	1.66 (dq, 13.2, 7.4)	29.3 t	1.84 (m)	27.3 t
	1.20 (overlap)		1.44 (m)		1.51 (dq, 13.2, 7.4)		1.65 (m)	
20	1.88 (m)	48.7 d	2.87 (m, overlap)	48.5 d	2.96 (m, overlap)	48.5 d	2.42 (m)	50.4 d
21		145.3 s		146.3 s		126.7 s		128.8 s
OMe	3.92 (3H, s)	55.7 q	3.90 (3H, s)	55.8 q	3.95 (3H, s)	55.8 q	4.06 (3H, s)	56.2 q

DOI: 10.1021/acs.orglett.9b01453
Org. Lett. 2019, 21, 4554–4558

unit consisting of C_{20}–C_{15}–C_{14}–C_3 (Figure 3, Unit B). Further, H-14 and H-16 showed the connectivity in the ^{1}H–^{1}H COSY spectrum. The signal of H-3 showed correlations to C-21 and C-5 in the HMBC spectrum, indicating connection between both units A/B via N-4/C-3. Additionally, H-16 and H-17 showed the HMBC correlations to C-2, disclosing another connection via C-2/16. Thus, the planar structure of alkaloid **1** was deduced from the interpretation of the obtained data.

The UV spectra of **2** displayed a better conjugated system from its absorption maxima at 245, 280, 342, and 400 nm. Comparison of both ^{13}C NMR data (Table 1) showed that **2** and **1** possessed nearly identical core structures. Obvious differences between both alkaloids were that compound **2** showed double bond signals (δ_C 137.7, 130.8) instead of two sp^3 signals (δ_C 49.3, 83.2) in **1**. The presence of new sp^2 proton signal δ_H 6.49 (d, J = 2.3 Hz) in the ^{1}H NMR spectrum of **2** was consistent with the double bond between C-16/17. This was supported by the HMBC correlations from δ_H 6.49 to signals of δ_C 48.5 (C-20), 37.2 (C-15), and 45.2 (C-14). The positive HRESIMS spectrum of alkaloid **2**[13] gave the molecular formula $C_{20}H_{22}N_2O$ with 11 degrees of unsaturation by m/z 307.1807 $[M + H]^+$. Compared to alkaloid **1**, the molecular mass of **2** was 18 Da less than that of **1**. These data suggested that **2** was a dehydrated derivative of **1**.

Taberbovine B (**3**)[14] was assigned a molecular formula of $C_{20}H_{20}N_2O$ on the basis of its HRESIMS data (m/z 305.1649 $[M + H]^+$, calcd 305.1648), which was two hydrogen atoms less than **2**. The ^{13}C NMR spectrum (Table 1) of **3** showed high similarity to that of **2**, except for the disappearance of two methylenes (δ_C 55.8 and 28.3) and the presence of an additional double bond (δ_C 128.9 and 101.6), which revealed that compound **3** was a dehydrogenated derivative of **2**. This deduction was further confirmed by the HMBC cross-peaks of H-3 (δ_H 4.74) with C-5 (δ_C 128.9), H-5 (δ_H 7.47), and H-6 (δ_H 7.01) with both C-7 (δ_C 129.1) and C-21 (δ_C 126.7).

Alkaloid **4**[15] showed a similar UV pattern to **2**. However, the absorption of UV light of the peak at 398 nm of **4** was much stronger than that of **2** at 400 nm, suggesting an additional electrophilic group in **4**. The HRESIMS of **4** exhibited the molecular formula $C_{20}H_{18}N_2O_3$ (m/z 357.1206 $[M + Na]^+$, calcd 357.1210), with 13 degrees of unsaturation. Its ^{1}H NMR spectrum (Table 1) indicated a similar quinoline core as in compounds **1**–**3**. In addition, two new coupling protons at δ_H 8.08 (d, J = 3.4 Hz) and at δ_H 7.52 (d, J = 3.4 Hz) downfield were present. The ^{13}C NMR and DEPT data (Table 1) of **4** showed 20 resonance signals, including nine sp^2 carbons (δ_C 160.4, 158.4, 152.8, 142.6, 139.5, 135.7, 128.8, 128.1, 126.3), five sp^2 methines (δ_C 133.1, 124.9, 121.2, 109.6, 103.3), two sp^3 methines (δ_C 80.8, 50.4), two methylenes (δ_C 34.9, 27.3), one methyl (δ_C 12.7), and one methoxy (δ_C 56.2). Compared to **1**, compound **4** exhibited five additional sp^2 carbons and a more extended conjugated system which was in agreement with its UV absorption. In the ^{1}H–^{1}H COSY spectrum of **4**, the correlation between δ_H 8.08 (H-5) and δ_H 7.52 (H-6) as well as their identical coupling constants (J = 3.4 Hz) indicated a double bond between C-5/6. Additionally, this presumption was supported by the HMBC correlations from both protons to C-21 (δ_C 128.8 s). In the HMBC spectrum, H-15 at δ_H 3.21 and at 2.50 showed cross-peaks to δ_C 152.8 (s), 139.5 (s), C-17 (δ_C 80.8, d), and C-19 (δ_C 27.3, t), assigning two carbon signals to C-16 and C-14, respectively. Thus, the double bond was located at C-16/14, which is conjugated to the carbonyl at C-3.

The relative configurations of the newly isolates were determined by ROESY correlations. In **1**–**3**, the ROESY cross-peaks between H-15β with both H-14 and H-20 assigned themselves at β-orientation. Furthermore, correlations of H-14/16, H-17/19 of **1** attributed them to be the same at β,α-orientation, respectively (Figure 4). Additionally, the large

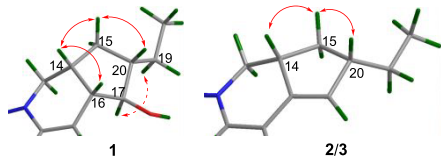

Figure 4. Key REOSY correlations of alkaloids **1**–**3**.

coupling constants of H-17 (t = 8.3 Hz) suggested that the dihedral angles between H-17/20 and H-17/16 were nearly 180°. Moreover, the ^{13}C chemical shifts of (14*R*,16*S*,17*R*,20*S*)-**1a** and its possible epimers **1b**–**1d** (SI) were calculated by the density functional theory (DFT) gauge independent atomic orbital (GIAO) method.[16] The experimental NMR data of **1** were compared with those calculated of **1a**–**1d** using the linear correlation coefficients (R2), root-mean-square deviation (RMSD), mean absolute deviation (MAD), corrected mean absolute deviation (CMAD), and DP4+ probability analysis.[17] The calculated ^{13}C NMR data for **1** possessed the highest R^2 value and lowest RMSD, MAD, and CMAD values (SI). In addition, DP4+ analysis based on all NMR data also showed **1** as the correct structure with 100% probability (Figure 5).

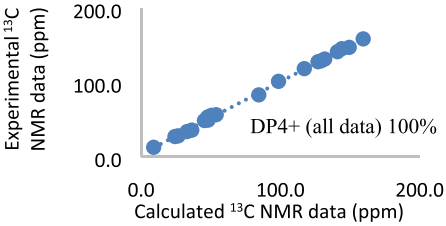

Figure 5. Correlation plots of experimental and calculated ^{13}C NMR for **1** and DP4+ results of of all NMR data.

NMR predicted data of **3** were calculated by the same method, but there was no remarkable difference between its possible epimers **3a**–**3d** (SI). Subsequently, ECD cacula-tions[18] of the **3a**–**3d** (SI) showed that the theoretical ECD curve for **3a** in the four candidate configurations (**3a**–**3d**) was identical with the experimental one for **3** (Figure 6).

The skeleton of **1**–**4** was confirmed by the X-ray crystal diffractions of **2**[19] and **4**.[20] The absolute configurations of **2** and **4** were determined as 14*R*,20*S* and 17*R*,20*S*, respectively (Figure 7). Based on the above analysis and biosynthesis theory, the absolute configurations **1** and **3** were elucidated as 14*R*,16*S*,17*R*,20*S* and 14*R*,20*S*, respectively. All four alkaloids were named as taberbovines A–D, respectively.

Though alkaloids **1**–**4** possessed similar UV–vis spectra to camptothecin analogues, however, their carbon skeletons were entirely different. By comparison to the known 14,15-didehydroaspidospermidine, we could propose that taberbo-vines A–D (**1**–**4**) were formed by decomposition and rearrangement from *Aspidosperma* type (Figure 8). 14,15-

DOI: 10.1021/acs.orglett.9b01453
Org. Lett. 2019, 21, 4554–4558

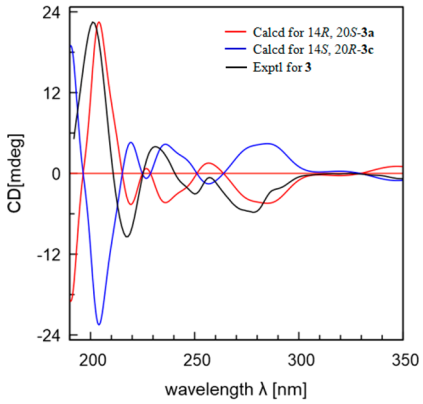

Figure 6. Experimental and calculated ECD spectra of **3** and its isomers.

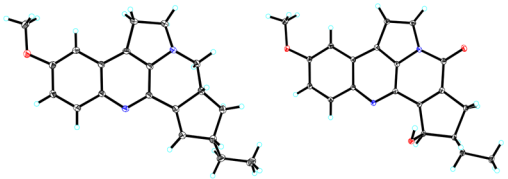

Figure 7. X-ray crystal diffraction of **2** (left) and **4** (right).

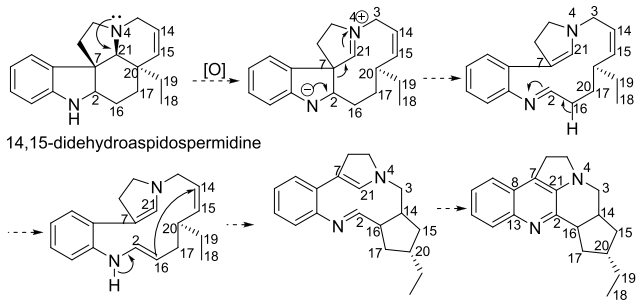

Figure 8. Possible biogenetic pathway of the skeleton of alkaloids **1**–**4**.

Didehydroaspidospermidine was usually distributed in the *Tabernaemontana*, *melodinus*, and other genus plants. First, 14,15-didehydroaspidospermidine was oxidized, simultaneously opening the bond of C–21/20 and forming an imine at position N_4=C_{21}. Subsequently, electrons of the imine transferred, producing an enamine (N_4–C_{21}=C_7) and an imine of N_1=C_2. Then, the imine of N_1=C_2 could be rearranged to an enamine N_1–C_2=C_{16}. Subsequently, an intramolecular electrophilic addition in the intermediate from C-16 to C-14 led to a new five-membered ring. Finally, a 6π electrocyclic reaction may take place between the two double bonds of C-7/21 and N-1/C-2 and two six-membered rings were formed. This step may lead to the skeleton with a 6/6/5/6/5 ring system of **1**–**4**. Afterward, oxygenation and addition reactions in this skeleton gave carbonyl, double bonds, and hydroxyl substitution, respectively. The compound numbering system corresponded in biogenetic origin to the monoterpenoid indole alkaloids.

Compounds **1**–**4** were also evaluated for their cytotoxicity. However, no effects could be observed at the concentration of 20 μM. All three compounds exhibited moderate inhibitory activities against nitric oxide (NO) production in LPS-activated RAW264.7 macrophages, with IC_{50} values of 5.2, 4.6, 4.4, and 3.3 μM, respectively (Positive control MG-132, IC_{50} = 0.21 μM).

As a new type of MQAs, taberbovines A–D with a multiring system would attract much attention from both chemists and biologists, and further studies such as in-depth biological tests are warranted.

■ ASSOCIATED CONTENT

Supporting Information

The Supporting Information is available free of charge on the ACS Publications website at DOI: 10.1021/acs.orglett.9b01453.

1D and 2D NMR, MS spectra, X-ray diffractions and ECD, NMR calculations of **1**–**4** (PDF)

Accession Codes

CCDC 1911621 and 1911623 contain the supplementary crystallographic data for this paper. These data can be obtained free of charge via www.ccdc.cam.ac.uk/data_request/cif, or by emailing data_request@ccdc.cam.ac.uk, or by contacting The Cambridge Crystallographic Data Centre, 12 Union Road, Cambridge CB2 1EZ, UK; fax: +44 1223 336033.

■ AUTHOR INFORMATION

Corresponding Author

*E-mail: xhcai@mail.kib.ac.cn.

ORCID

Johann Schinnerl: 0000-0003-4494-8736
Xiang-Hai Cai: 0000-0002-6723-6988

Notes

The authors declare no competing financial interest.

■ ACKNOWLEDGMENTS

This project was supported in part by the Applied Basic Research Project of Yunnan Province (No. 2016FA030) and National Natural Science Foundation of China (31370377). Computational resources used in this work were supported in part by SciGrid, Chinese Academy of Science. We also thank Zhao S. M. of ShanghaiTech University for his efforts in bioactivity testing.

■ REFERENCES

(1) Ziegler, J.; Facchini, P. J. *Annu. Rev. Plant Biol.* **2008**, *59*, 735–769.
(2) Stoeckigt, J.; Panjikar, S. *Nat. Prod. Rep.* **2007**, *24*, 1382–1400.
(3) Zhang, B. J.; Yan, J. M.; Wu, Z. K.; Liu, Y. P.; Bao, M. F.; Cheng, G. G.; Luo, X. D.; Cai, X. H.; Li, Y. *Helv. Chim. Acta* **2013**, *96*, 2288–2298.
(4) Cai, X. H.; Li, Y.; Su, J.; Liu, Y. P.; Li, X. N.; Luo, X. D. *Nat. Prod. Bioprospect.* **2011**, *1*, 25–28.
(5) Liu, Y. P.; Li, Y.; Cai, X. H.; Li, X. Y.; Kong, L. M.; Cheng, G. G.; Luo, X. D. *J. Nat. Prod.* **2012**, *75*, 220–224.
(6) Peubelocou, N.; Potier, P.; Plat, M.; Koch, M. *Phytochemistry* **1972**, *11*, 2109–2111.
(7) Li, P. T.; Leeuwenberg, A. J. M.; Middleton, D. J. *Flora of China* **1995**, *16*, 153.
(8) Hirasawa, Y.; Miyama, S.; Hosoya, T.; Koyama, K.; Rahman, A.; Kusumawati, I.; Zaini, N. C.; Morita, H. *Org. Lett.* **2009**, *11*, 5718–5721.
(9) (a) Liu, B.; Liu, S. J.; Zhan, R.; Huang, G. L.; Tian, X. J.; Chen, Y. G. *Chem. Nat. Compd.* **2018**, *54*, 814–817. (b) Lien, T. P.; Ripperger, H.; Porzel, A.; Merzweiler, K.; Sung, T. V.; Adam, G. *Phytochemistry* **1998**, *49*, 1457–1461. (c) Lien, T. P.; Kamperdick, C.;

DOI: 10.1021/acs.orglett.9b01453
Org. Lett. 2019, 21, 4554–4558

Van Sung, T.; Adam, G.; Ripperger, H. *Phytochemistry* **1998**, *49*, 1797−1799.
(10) Pirillo, A.; Verotta, L.; Gariboldi, P.; Torregiani, E.; Bombardelli, E. *J. Chem. Soc., Perkin Trans. 1* **1995**, 583−587.
(11) Taberbovine A (**1**): yellow powder; $C_{20}H_{24}N_2O_2$; $[\alpha]_{20}^{D}$ = +15 (*c*, 0.05, CH_3OH); UV (CH_3OH) λ_{max} (log ε) 224 (4.45), 261 (4.41), and 357 (3.90) nm; ^1H (800 Hz) and ^{13}C (200 Hz) NMR data (acetone-d_6), Table 1; Positive ESIMS *m*/*z* 325 $[M + H]^+$. HRESIMS (*m*/*z* 325.1908 $[M + H]^{+\bullet}$, calcd for $C_{20}H_{25}N_2O_2$, 325.1911).
(12) Tagami, K.; Nakazawa, N.; Sano, S.; Nagao, Y. *Heterocycles* **2000**, *53*, 771−775.
(13) Taberbovine B (**2**): yellow prism crystal; $C_{20}H_{22}N_2O$; $[\alpha]_{20}^{D}$ = −161 (*c*, 0.05, CH_3OH); UV (CH_3OH) λ_{max} (log ε) 245 (4.44), 280 (4.48), 342 (3.83), and 400 (3.88) nm; ^1H (800 Hz) and ^{13}C (200 Hz) NMR data (acetone-d_6), Table 1; Positive ESIMS *m*/*z* 307 $[M + H]^{+\bullet}$. HRESIMS (*m*/*z* 307.1807 $[M + H]^+$, calcd for $C_{20}H_{23}N_2O$, 307.1805).
(14) Taberbovine C (**3**): yellow powder; $C_{20}H_{20}N_2O$; $[\alpha]_{20}^{D}$ = −41.0 (*c*, 0.11, CH_3OH); UV (CH_3OH) λ_{max} (log ε) 218 (4.39), 252 (4.46), 281 (4.38), 350 (4.22), and 365 (4.27) nm; ^1H (400 Hz) and ^{13}C (125 Hz) NMR data (acetone-d_6), Table 1; Positive ESIMS *m*/*z* 305 $[M + H]^{+\bullet}$, HRESIMS *m*/*z* 305.1649 $[M + H]^+$ (calcd for $C_{20}H_{21}N_2O$, 305.1648).
(15) Taberbovine D (**4**): yellow prism crystal; $C_{20}H_{18}N_2O_3$; $[\alpha]_{20}^{D}$ = −58 (*c*, 0.03, CH_3OH); UV (CH_3OH) λ_{max} (log ε) 230 (4.48), 275 (3.97), 287 (4.01), and 398 (4.03) nm; ^1H (800 Hz) and ^{13}C (200 Hz) NMR data (acetone-d_6), Table 1; Positive ESIMS *m*/*z* 335 $[M + H]^{+\bullet}$, HRESIMS *m*/*z* 357.1206 $[M + Na]^+$ (calcd for $C_{20}H_{18}N_2O_3Na$, 357.1210).
(16) Lodewyk, M. W.; Siebert, M. R.; Tantillo, D. *Chem. Rev.* **2012**, *112*, 1839−1862.
(17) Grimblat, N.; Zanardi, M. M.; Sarotti, A. M. *J. Org. Chem.* **2015**, *80*, 12526−12534.
(18) Pescitelli, G.; Bruhn, L. *Chirality* **2016**, *28*, 466−474.
(19) Crystal data for **2**: $C_{20}H_{22}N_2O{\cdot}H_2O$, *M* = 324.41, *a* = 16.6710(3) Å, *b* = 7.17490(10) Å, *c* = 13.9729(3) Å, α = 90°, β = 90°, γ = 90°, *V* = 1671.34(5) Å^3, *T* = 107.(2) K, space group *P*21212, *Z* = 4, μ(Cu Kα) = 0.662 mm^{-1}, 16 906 reflections measured, 3313 independent reflections (R_{int} = 0.0343). The final R_1 values were 0.0354 ($I > 2\sigma(I)$). The final $wR(F^2)$ values were 0.1206 ($I > 2\sigma(I)$). The final R_1 values were 0.0373 (all data). The final $wR(F^2)$ values were 0.1249 (all data). The goodness of fit on F^2 was 1.109. Flack parameter = 0.00(9). The CCDC deposit number is 1911621.
(20) Crystal data for **4**: $C_{20}H_{18}N_2O_3$, *M* = 334.36, *a* = 4.5026(4) Å, *b* = 15.0542(12) Å, *c* = 11.6292(10) Å, α = 90°, β = 98.515(3)°, γ = 90°, *V* = 779.57(11) Å^3, *T* = 100.(2) K, space group *P*1211, *Z* = 2, μ(Cu Kα) = 0.787 mm^{-1}, 13 108 reflections measured, 3071 independent reflections (R_{int} = 0.0311). The final R_1 values were 0.0281 ($I > 2\sigma(I)$). The final $wR(F^2)$ values were 0.0888 ($I > 2\sigma(I)$). The final R_1 values were 0.0282 (all data). The final $wR(F^2)$ values were 0.0894 (all data). The goodness of fit on F^2 was 0.851. Flack parameter = 0.02(5). The CCDC deposit number is 1911623.

NOTE ADDED AFTER ASAP PUBLICATION

NMR values were revised in Table 1 and the text, and the SI file was corrected on June 12, 2019.

DOI: 10.1021/acs.orglett.9b01453
Org. Lett. 2019, 21, 4554−4558